

Cu-induced changes in properties of the arsenic chalcogenides

© N. Bollé, P. Hertogen, G.J. Adriaenssens, C. Sénémaud*, A. Gheorghiu-de La Rocque*

K.U. Leuven, Laboratorium voor Halfgeleiderfysica, Celestijnenlaan 200D,
B3001 Heverlee, Belgium

* Université Pierre et Marie Curie, Laboratoire de Chimie-Physique, UMR CNRS 7614,
75231 Paris, cedex 05, France

(Получена 16 февраля 1998 г. Принята к печати 2 марта 1998 г.)

The influence of the presence of between 1% and 6% of Cu in arsenic chalcogenide glasses is examined through a study of the electronic energy levels by means of X-ray photoelectron and X-ray emission spectroscopy, through an investigation of the low-energy tunneling systems by means of phonon echoes at 0.37 K, and through an examination of the photodarkening and the photoinduced dichroism caused by polarized Ar⁺-laser irradiation. Possible links between the various effects are being looked for. The Cu atoms do become an integral part of the amorphous lattice structure and strongly influence the photodarkening, but they do not have a significant effect on the tunneling systems or the dichroism. It is concluded that the tunneling levels and the dichroism involve only local configurations, while the photodarkening involves larger-scale areas of the lattice.

1. Introduction

Almost from the beginning of the study of vitreous chalcogenide semiconductors in the Laboratory of Professor Kolomiets, the effects of adding both non-metallic and metallic elements to the glasses were investigated. This early interest was undoubtedly generated by the desire to find appropriate dopants for the amorphous semiconductors, and it explains why most attention was being paid to the changes in electrical properties of the samples. A review of these results can be found in ref. [1]. Subsequently, the interest in the chalcogenides shifted to their optical properties, especially their ability to sustain reversible photoinduced changes to these properties [2]. Much attention was paid to the photoinduced shifts of the optical absorption edge of the glasses [3], the so-called photodarkening and photobleaching, and later to the optical anisotropies that are induced by polarized light beams [4]. These two types of effects have become known as the scalar and vectoral phenomena. These photoinduced changes in the optical parameters were found to be the result of structural changes in the amorphous lattice [5] that can even result in macroscopic deformations of the chalcogenide materials [6]. A wide range of models has already been proposed to account for the effects, but most deal with part of the observations only. Consequently, and although some models do attempt to link scalar and vectoral effects, not a single one of those models has, so far, been able to obtain widespread agreement. Recent surveys of both the experimental observations and the proposed models have been given by Shimakawa, Kolobov and Elliot [7] and by Tanaka [8]. From an examination of those reviews it becomes clear that more experimental data will be required to make some progress in resolving the physical mechanisms behind the photoinduced structural changes.

In this paper, we therefore explore the influence on both the electronic structure and the photoinduced effects of introducing small concentrations of Cu into the arsenic chalcogenide glasses. It is known that the presence of 1%

Cu in bulk As₂S₃, or 5% Cu in bulk As₂Se₃, eliminates the photodarkening that is normally observed in those materials [9]. Such Cu-modified compounds should hence be good candidates for studying the structure of the glasses, as revealed by X-ray-induced photoelectron spectroscopy (XPS) and X-ray emission spectroscopy (XES), in relation to the appearance or disappearance of the photodarkening. The same samples can also be used to test the links that have been suggested [10] between, on the one hand, the centers that are responsible for the photodarkening and, on the other hand, the soft potential sites of the lattice that give rise to the low-temperature anomalies in the phonon spectrum of amorphous materials. The latter can be identified through the low-energy tunneling states (TS) that can be detected in a backward-wave phonon echo (BWE) experiment at 0.4 K. Such BWEs from Cu-free and Cu-containing samples will be compared. Finally, we will also examine the relationship of scalar to vectoral photoinduced effects in the light of the Cu influence on the photodarkening.

2. Experimental techniques

Bulk samples of Cu-modified As₂S₃ or As₂Se₃ were prepared by the standard procedure of melt quenching after alloying of the pure compounds with copper at 900°C for 20 hours in a rocking furnace. A few samples prepared in the group of Prof. P.C. Taylor at the University of Utah were used for comparison; no differences were observed. Films for optical measurements were prepared for some compositions by thermal evaporation of the ground compound.

2.1. X-ray photoelectron and X-ray emission spectroscopies

XPS and XES are complementary techniques for obtaining information on the electronic structure of our amorphous compounds [11]. From XPS we determine the energy levels of the core electrons and the global energy distribution of the valence band states, while XES provides information

concerning the bonding arrangements of valence electrons around a particular atomic site.

For this study we have analyzed the XPS spectra of the S $2p$ and As $3p, 3d$ core levels, and we obtained the total valence band states (VB) modulated by the photoionisation cross sections. The spectra were excited by means of a standard Mg K_{α} X-ray source with $h\nu = 1253.6$ eV. In our experiment, the total instrumental broadening is estimated to be 0.6 eV for core levels and 1.0 eV for VB. The core level spectra are scanned with a 0.1 eV step and the XPS VB data with a 0.2 eV step. In the case of non-conductive samples, such as the arsenic chalcogenides, a charging effect of the sample can be observed in the data. In order to take this effect into account, we calibrate the binding energy scale by reference to the C $1s$ line observed from hydrocarbonated species which are always present at the surface of the sample. The C $1s$ line is set at 285.0 eV. The interpretation of the core level lines is based on a reconstruction of each spectral distribution into Voigt functions. In the case of the valence band, the spectra are superimposed on a background due to the inelastic electron scattering; no correction for this effect was undertaken, and therefore the spectra contain a non-constant background. It may be mentioned that the sample thickness which contributes to the XPS spectra is limited by the mean free path of the electrons and can be estimated to be 1–3 nm for the present cases.

The XES measurements concern S K_{β} band corresponding to the electronic transition $3p \Rightarrow 1s$. They are analyzed by means of a cylindrical bent-crystal vacuum spectrometer (radius: 250 mm). The monochromator is a $10\bar{1}1$ quartz crystal ($2d = 0.66855$ nm) used in first order reflection. The spectra are excited with a 5 kV, 5 mA electron beam, and the detector is a proportional Ar/CH₄ counter. The energy resolution of the instrument is estimated to be 1.0 eV [12]. The X-ray spectra are measured as a function of the photon energy corresponding to the transition $E(S 1s) - E(S 3p)$. On this energy scale, the Fermi level position corresponds to the binding energy $E(S 1s)$; it is obtained by combining the XPS data for the S $2p_{3/2}$ binding energy and the XES determination of the S $K_{\alpha_{1,2}}$ ($2p_{1/2,3/2} - 1s$) X-ray transition energy. Then $E_F(S 1s) = E(S K_{\alpha_1}) + E(S 2p_{3/2})$. Consequently the XPS and XES spectra can be obtained on a common energy scale with the Fermi level as reference point.

2.2. Backward-wave echoes

In a backward-wave echo experiment two microwave pulses, separated by a time τ , are applied to the sample in a re-entrant cavity. Via the surface excitation method a forward-propagating hypersonic wave is generated by the first pulse. (A coating of ZnO powder suspended in glyptol varnish is used in our experiments as a piezoelectric transducer). Through the interaction between the hypersonic wave and the microwave electric field of the second pulse at some non-linear entities, a reversal of the wave vector

($\mathbf{k} \rightarrow -\mathbf{k}$) is induced. At time 2τ this backward propagating wave reaches the transducer again and gives rise to an echo.

In chalcogenides the non-linear coupling between the electric field and the acoustic wave is due to the tunneling systems present in these materials. Indeed, post studies have indicated that TS do act as such non-linearities [13]. Experimentally, the intensity of the echo will increase with increasing intensity, I_a , of the acoustic wave until the TS become saturated, i.e. the populations of the tunneling levels have been equalized at the critical acoustic intensity, I_{ca} . Theoretical considerations [14] then allow us to distinguish two regions in the behavior of the echo intensity I_E as a function of the incident power P_m , depending on the value of $Y_a = I_a/I_{ca}$:

1. If $Y_a \ll 1$ (TS are unsaturated) then $I_E \sim P_m^3$.

2. If $Y_a \gg 1$ (TS are saturated) then I_E is independent of the incident power; I_E shows a plateau, where the saturation value P_{ex} is a measure of the number of tunneling states in the sample.

We have measured the input power dependence of the backward-wave echo power in pure and Cu-modified As₂S₃ and As₂Se₃ compounds. The bulk samples were prepared from melt-quenched glasses out of which cylindrical samples of 3 mm diameter by 10 mm length were drilled to fit the cylindrical microwave cavity. Our measurements were carried out at a frequency of 9.3 GHz and at a constant temperature of 0.37 K. Since the tunneling systems envisioned here are indeed those of the soft-potential model (SPM) that has been deduced from the low-temperature anomalies which are characteristic of all glasses [15], we have to study them below 1 K to obtain sufficient sensitivity.

2.3. Photodarkening and photoinduced dichroism

The 514.5 nm beam of a polarized Ar⁺-laser was used for measuring the photoinduced optical effects. Relative changes in optical transmission caused by the illumination were recorded to compare the degree of photodarkening in both unmodified and Cu-containing samples. Values for the linear photoinduced dichroism, this is the difference in optical absorption coefficients $\alpha_{\perp} - \alpha_{\parallel}$, where $\alpha_{\perp, \parallel}$ are the absorption coefficients in the direction perpendicular to, and parallel with the direction of the polarization of the inducing beam, were obtained by measuring transmitted light intensities I_{\perp} and I_{\parallel} by standard lock-in detection techniques when the polarization of a probe beam is modulated between the parallel and orthogonal directions at a frequency of 1 kHz by means of an electrooptic modulator, and by then making use of the relation that was derived in [16]:

$$\alpha_{\perp} - \alpha_{\parallel} = \frac{I_{\parallel} - I_{\perp}}{h(I_{\parallel} + I_{\perp})/2}, \quad (1)$$

where h is the sample thickness.

3. Results

The addition of Cu to the arsenic chalcogenides did modify some characteristics, while leaving others unchanged. We will first summarize the results technique by technique before attempting an encompassing interpretation.

3.1. Electronic energy levels

The core levels S $2p$, As $3p$ and As $3d$ were examined by XPS for a pure As_2S_3 sample and for one which contained 6% of Cu. We observe practically no shift for the As lines, with $3p_{1/2}$ at 146.2 eV, $3p_{3/2}$ at 141.2 eV, and $3d_{5/2}$ at 41.7 eV. For S $2p_{1/2}$ (163.6 eV) and S $2p_{3/2}$ (162.5 eV), a broadening of the line is observed when Cu is added. This broadening is asymmetric and occurs towards the lower binding energies (BE). It reveals a shift of ~ 0.2 eV towards

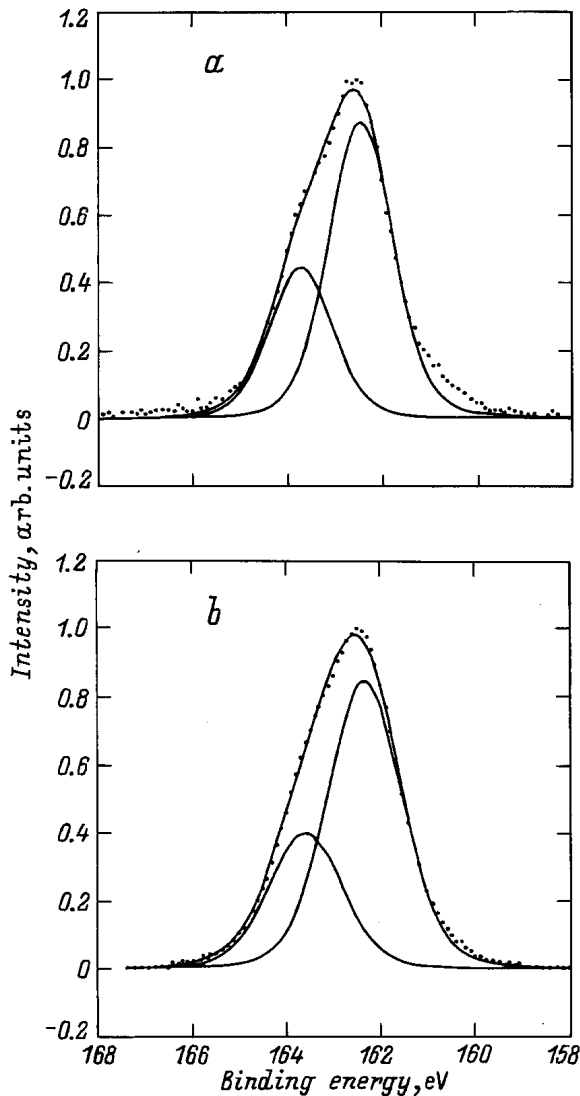


Figure 1. XPS binding energy spectrum of S $2p$ core electrons in (a) As_2S_3 and (b) $\text{Cu}_6(\text{As}_2\text{S}_3)_{94}$, together with a decomposition into their $2p_{1/2}$ and $2p_{3/2}$ components.

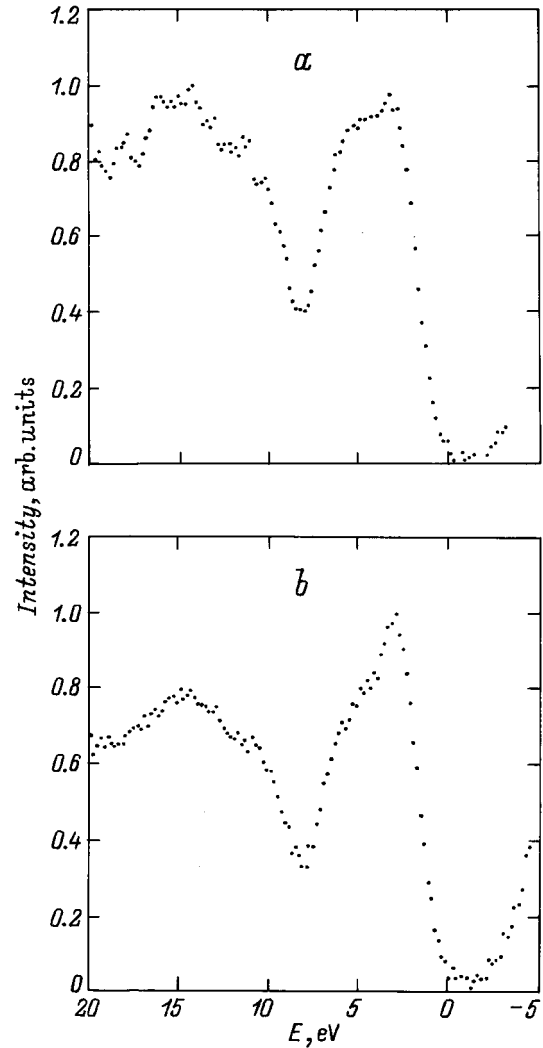


Figure 2. XPS valence band spectra from (a) As_2S_3 (b) $\text{Cu}_6(\text{As}_2\text{S}_3)_{94}$.

low BE with the presence of Cu. Fig. 1 shows the S $2p$ spectra and their decomposition into the spin-orbit splitted $2p_{1/2}$ and $2p_{3/2}$ lines.

The XPS valence band spectra observed for As_2S_3 and $\text{As}_2\text{S}_3(\text{Cu})$ are shown in Fig. 2. Both spectra exhibit a wide peak between E_F and about 8 eV, followed by a broad band from ~ 8 to ~ 17 eV. It is known [17] that the structure that is seen in the first peak of As_2S_3 consists of a leading feature at about 3 eV which is associated with the lone pair p electrons of the chalcogen atoms, and a second contribution centered around 6 eV which is related to the bonding p states. A strong minimum separates the p states of the first peak from the deeper-lying broad band which consists of s states and also shows some structure. In $\text{As}_2\text{S}_3(\text{Cu})$, the width of the p band is approximately the same as in As_2S_3 but strong modifications occur at the top of the valence band, with the 3 eV peak becoming more prominent. Differences in the s bands of As_2S_3 and $\text{As}_2\text{S}_3(\text{Cu})$ are less pronounced.

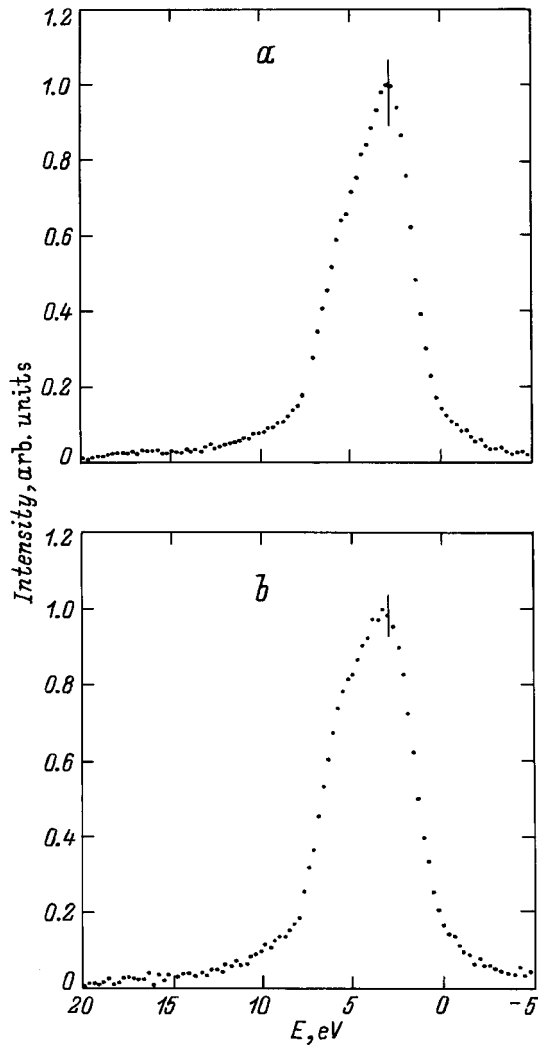


Figure 3. XES $S K_{\beta}$ spectra of the valence band $S 3p$ electrons in (a) As_2S_3 (b) $Cu_6(As_2S_3)_{94}$.

The $S 3p$ valence band states were also examined through the XES sulfur K_{β} spectrum. As explained in the previous section, these X-ray spectra were obtained in the BE scale with E_F as the origin. The results for both types of samples are shown in Fig. 3. The $S K_{\beta}$ spectrum exhibits an asymmetric distribution with the steep edge towards the low BE. The most prominent feature is again due to the lone pair electrons, while the adjoining shoulder on the high BE side marks the position of the bonding sulfur p states. These $S K_{\beta}$ spectra correspond to earlier ones reported [18] for As_2S_3 . For our two compositions the low BE edge is observed in the same energy position and the slope of the edge is the same. However, a significant broadening is observed at about 5 eV from E_F in the $As_2S_3(Cu)$ sample as compared to As_2S_3 .

3.2. Tunneling states

We have studied the BWEs from As_2Se_3 and $Cu_5(As_2Se_3)_{95}$ glasses as well as for As_2S_3 , $Cu_1(As_2S_3)_{99}$ and $Cu_{1.5}(As_2S_3)_{98.5}$ glasses. Fig. 4 and Fig. 5 show the

results of the measurements of the backward-wave echo power as a function of input power for the selenide and sulfide glasses respectively. The lowest echo powers given in both figures represent the minimum power that could be detected, and the other values are given relative to that one.

While the data sets are obviously not identical, no significant difference in the behaviour of the echopower as a function of input power can be seen between the Cu-modified and the unmodified chalcogenides. Most specifically: the saturation which is a signature of the presence of TS (and hence soft potentials) is equally prominent in all cases. However, the magnitude of the backward-wave echo depends on experimental factors such as the bonding of the transducer and the quality factor of the cavity. Since these are different for the different samples, the saturation value of the echopower P_{ex} , and together with that, the number of TS can, unfortunately, not be compared for the different samples. In fact, increasing Cu content does increase the conductivity of the samples, thereby decreasing the Q value of the cavity, to that extent that measurements become impossible. This happens sooner for the sulfur than for the selenium chalcogenides.

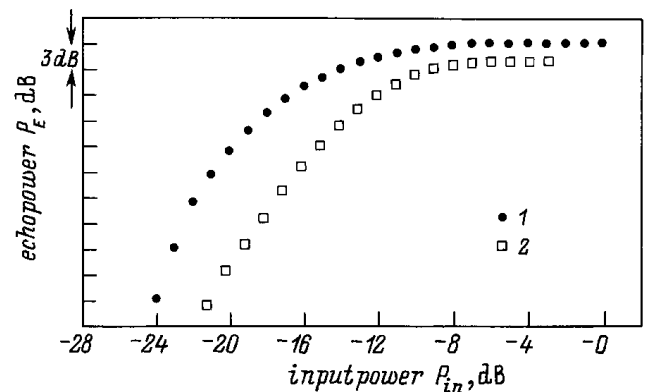


Figure 4. The BWE power as a function of the microwave power for the selenide glasses at 0.37 K: As_2Se_3 (1) and $Cu_5(As_2Se_3)_{95}$ (2). 0 dB corresponds to a peak power of 1.2 W.

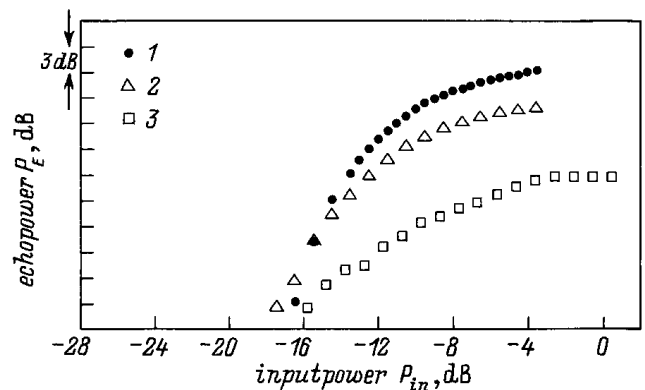


Figure 5. The BWE power as a function of the microwave power for the sulfide glasses at 0.37 K: As_2S_3 (1), $Cu_1(As_2S_3)_{99}$ (2) and $Cu_{1.5}(As_2S_3)_{98.5}$ (3). 0 dB corresponds to a peak power of 1.2 W.

3.3. Photoinduced changes

Thermally evaporated films were used for these measurements. The results reported here originate with a $2\ \mu\text{m}$ thick film evaporated from pure As_2S_3 and with a $3.8\ \mu\text{m}$ thick one prepared on the basis of $\text{Cu}_4(\text{As}_2\text{S}_3)_{96}$ glass. Progressive photodarkening under continuous illumination was measured for both films, unlike the observations on bulk glasses [9] where the 4% Cu would have prevented the photodarkening. It has already been reported, however, that in the corresponding evaporated films the photodarkening is not eliminated [19]. We, nevertheless, observe a clear difference between the two materials: while in the As:S films the measured transmission drops to below 10% of its initial value, the drop is only down to $\sim 30\%$ in the As:S:Cu films. These numbers both slightly decrease with increasing light-intensity. The photodarkening kinetics speed up in similar fashion for both types of films with more intense illumination.

The photoinduced dichroism was also measured for the above films, and here no significant differences could be observed. We found that the total, reversible variation in the dichroism, when the polarization direction of the inducing beam is changed between orthogonal directions, does not change by more than 10% amongst the various As:S and As:S:Cu films, in contrast with the photodarkening where the changes are stronger by a factor of 3 in films without Cu with respect to films which contain Cu.

4. Discussion

Some of the questions that were raised in the introduction are being answered directly by the results in the previous section. It does become clear, for instance, that photodarkening and photoinduced anisotropy do not have a common origin; the former is strongly influenced by the presence of Cu, the latter not in a significant way. Also the proposed link between centers that are responsible for the photostructural changes in the chalcogenide glasses and the soft atomic potentials that are implicated in the low-temperature anomalies can be ruled out. Indeed, the results for the backwardwave echo measurements confirm the presence of an essentially unchanged number of tunneling systems in a region where the photodarkening has disappeared from the bulk glasses. In other words, while the presence of Cu inhibits the photodarkening, it leaves other characteristic properties of the chalcogenide glasses such as the photoinduced anisotropy or the soft-potential sites unimpaired.

Our results from XPS, XES and BWE show that the Cu atoms do become an integral part of the amorphous lattice to form a real alloy. Indeed comparing the SK_β XES spectra of Fig. 3 with a corresponding one from CuS [20], we see that the added intensity near 6 eV in the As:S:Cu sample does agree with the position of the main $S3p$ density in the CuS bond. The changes in the distribution of p states in the valence band XPS spectra primarily result in a sharper

definition of the lone-pair component as is normally seen in chalcogen-rich compounds. This need not be interpreted as evidence for a somewhat increased density of S-S bonds (as would occur when the Cu would mostly bond to As), but probably just reflects the change in average bonding angle at the S when a Cu atom substitutes for As. From early EXAFS studies [21] we know that Cu is fourfold coordinated in the arsenic chalcogenide glasses, while a normal As site is of course only threefold coordinated.

When we take a closer look now at the BWE results, we notice that there is a decrease of the slope at low input powers for the Cu containing samples with respect to the standard chalcogenides. In a previous study [22] we found a correlation between these different slopes and the mean coordination number of the lattice. The third power (P_{in}^3) predicted by the theory holds for the compositions with mean coordination $\langle r \rangle \leq 2.4$. According to Thorpe [23], these networks are all floppy. The rigid samples, those with a higher value of $\langle r \rangle$, are found to have a lower slope and as a consequence the input power dependence of the echopower deviates from the theory. In addition, Thorpe predicts that the number of TS should be smaller in a rigid than in a floppy glass.

The BWE results presented here and the lower slope of the Cu-containing samples thus agree with a fourfold coordination of the Cu atoms, which results in a higher average lattice coordination. The effect on the average coordination of Group I metals such as Cu is described by a general model proposed by Liu and Taylor [24] for a wide range of semiconducting glasses including the As:Se and As:S systems. Their model for the bonding in glasses, is based on analogies with bonding in minerals of the Cu:As:S system. In these minerals Cu is fourfold coordinated, As threefold coordinated for low enough Cu concentration ($x < 31.6\%$) and S is either twofold or fourfold coordinated. Further on, only Cu-S and As-S bonds are present. Liu and Taylor assume that the same rules hold for the Cu:As:S and Cu:As:Se glasses. They calculated the coordination number for glasses in the systems $\text{Cu}_x(\text{As}_{0.4}\text{Se}(\text{S})_{0.6})_{1-x}$ and the following relation was found: $\langle r \rangle = 2.4 + 4.6x$. The excellent agreement of the predictions for the average coordination number with X-ray radial distribution data [25] confirms that the local bonding configurations are very well understood. Using this prediction, the average coordination of our Cu-modified samples will be larger than 2.4, which means that the samples are rigid. This confirms our interpretation for the reduced slope of the echopower as function of input power found in these materials. Remark that the decrease of the slope appears at a smaller concentration of Cu atoms for the sulfide than for the selenide glasses. This is not surprising because the same effect is seen for other phenomena such as the photodarkening and the conductivity of these systems.

It is widely assumed that the arsenic chalcogenide glasses do still exhibit much of the layered structure of their crystalline phase in the amorphous one. However, fourfold coordinated Cu atoms could easily link adjacent layers and thus modify the characteristics of the glass. Exactly such

effect has recently been proposed by Shimakawa et al. [26] to explain the role of Cu in the inhibiting of photodarkening, which in their model is related to a relative sliding motion of adjoining lattice planes. Other phenomena which would not depend on that motion should then not be affected by the presence of the Cu cross-links. That would be the case for the photoinduced anisotropy, where the intrinsic charged defects of the chalcogenide glasses have been proposed as the active elements [27], and for the soft potential sites that generate the tunneling systems seen through the low-temperature BWEs.

5. Conclusions

Our XPS and XES measurements have confirmed that Cu atoms added to the arsenic chalcogenide glasses do become an integral part of the amorphous lattice, and our low-temperature phonon studies show a concomitant increase in average lattice coordination in agreement with fourfold Cu coordination. From the fact that Cu levels which eliminate photodarkening in As_2S_3 or As_2Se_3 , leave the vectoral photoinduced anisotropy or the density of low-energy tunneling states intact, we conclude that the photodarkening must be related to the chalcogenide network as a whole, and not to the specific defect configurations or soft potentials which are implicated in the anisotropy phenomena or in the low-temperature anomalies.

However, the most obvious conclusion of all the above considerations must undoubtedly be that more than 35 years after the beginning of chalcogenide semiconductor research by Kolomiets and his co-workers, we are still far removed from a comprehensive understanding of these fascinating materials.

Acknowledgment

This research was supported by the French–Flemish TOURNESOL scientific collaboration program.

References

- [1] B.T. Kolomiets, V.L. Averyanov, V.M. Lyubin, O.J. Prikhokdo. *Sol. Energy Mater.*, **8**, 1 (1982).
- [2] B.T. Kolomiets, V.M. Lyubin. *Mater. Res. Bull.*, **13**, 1343 (1978).
- [3] V.L. Averyanov, A.V. Kolobov, B.T. Kolomiets, V.M. Lyubin. *Phys. St. Sol. (a)*, **57**, 81 (1980).
- [4] V.G. Zhdanov, B.T. Kolomiets, V.M. Lyubin, V.K. Malinovskii. *Phys. St. Sol. (a)*, **52**, 621 (1979). V.M. Lyubin, V.K. Tikhomirov. *J. Non-Cryst. Sol.*, **144**, 133 (1989).
- [5] K. Tanaka. *Sol. St. Commun.*, **15**, 1521 (1974).
- [6] H. Hisakuni, K. Tanaka. *Appl. Phys. Lett.*, **65**, 2925 (1994); P. Kremer, A.M. Moulin, R.J. Stephenson, T. Rayment, M.E. Welland, S.R. Elliott. *Science*, **277**, 1799 (1997).
- [7] K. Shimakawa, A. Kolobov, S.R. Elliott. *Adv. Phys.*, **44**, 475 (1995).
- [8] K. Tanaka. *Current Opinion in Sol. St. & Mater. Sci.*, **1**, 567 (1996).
- [9] J.Z. Liu, P.C. Taylor. *Phys. Rev. Lett.*, **59**, 1938 (1987).
- [10] M.I. Klinger. *Phys. Reports*, **165**, 275 (1988); M. Klinger. *J. Non-Cryst. Sol.*, **137 & 138**, 939 (1991).
- [11] C. S  nemaud. *J. Non-Cryst. Sol.*, **198–200**, 85 (1996).
- [12] S. Dupont, A. Gheorghiu, C. S  nemaud, J.-M. Mariot, C.F. Hague, P.E. Lippens, J. Olivier-Fourcade, J.-C. Jumas. *J. Phys.: Condens. Matter*, **8**, 8421 (1996).
- [13] N. Vanreyten, L. Michiels. *Phys. Rev. B*, **37**, 9079 (1988).
- [14] L. Michiels, N. Vanreyten. *J. Phys. C: Sol. St. Phys.*, **21**, 4629 (1988).
- [15] D.A. Parshin. *Phys. Rev. B*, **49**, 9400 (1994).
- [16] V.M. Lyubin, V.K. Tikhomirov. *Fiz. Tverd. Tela*, **32**, 1838 (1990). *Sov. Phys. Sol. St.*, **32**, 1069 (1990).
- [17] S.G. Bishop, N.J. Shevchik. *Phys. Rev. B*, **12**, 1567 (1975).
- [18] G. Leonhardt, H. Neumann, A. Kosakov, T. G  tze, M. Petke. *Physica Scripta*, **16**, 448 (1977).
- [19] J.Z. Liu, P.C. Taylor. *J. Non-Cryst. Sol.*, **97 & 98**, 1123 (1987).
- [20] V.I. Anisimov, V.A. Gubanov, E.Z. Kurmaev. *J. Struct. Chem.*, **21**, 291 (1981).
- [21] S. Hunter, A. Bienenstock. In: *Structure and properties of non-crystalline semiconductors*. Ed. by B.T. Kolomiets (Academy of Sciences, A.F. Ioffe Institute, Leningrad, 1976) p. 151.
- [22] N. Boll  , L. Michiels, G.J. Adriaenssens. *J. Non-Cryst. Sol.* (in press).
- [23] M.F. Thorpe. *J. Non-Cryst. Sol.*, **57**, 355 (1983).
- [24] J.Z. Liu, P.C. Taylor. *Sol. St. Commun.*, **70**, 81 (1989).
- [25] K.S. Liang, A. Bienenstock, C.W. Bates. *Phys. Rev. B*, **10**, 1528 (1974).
- [26] K. Shimakawa, N. Yoshida, A. Ganjoo, Y. Kuzukawa, J. Singh. *Phil Mag. Lett.*, **77**, 153 (1998).
- [27] G.J. Adriaenssens, V.K. Tikhomirov, S.R. Elliott. *J. Non-Cryst. Sol.* (in press).

Редактор В.В. Чалдышев